Adsorption of Copper(II) from Aqueous Solution by Mg/Fe-Layered Double Hydroxide

N. Ayawei[1,*], A.O. Osikoya[3], A.T. Ekubo[2], D. Wankasi[3] and E.D. Dikio[3,*]

[1]Department of Chemical Sciences, Niger Delta University, Wilberforce Island, Bayelsa State, Nigeria
[2]Department of Chemistry, Federal University of Technology, Otuoke, Bayelsa State, Nigeria
[3]Applied Chemistry and Nanoscience Laboratory, Department of Chemistry, Vaal University of Technology, P. O. Box X021, Vanderbijlpark, South Africa

*Corresponding authors: E-mail: ayawei4acad@gmail.com; ezekield@vut.ac.za

Layered double hydroxide (LDH), of Mg/Fe ratio 2:1 was synthesized by co-precipitation method and characterized using X-ray diffraction, Fourier transform infrared spectroscopy and field emission scanning electron microscopy/energy-dispersive X-ray spectroscopy (FESEM/ EDX). The effects of time, concentration and temperature on the adsorption Cu^{2+} by the layered double hydroxide were studied. The Freundlich and Langmuir isotherms were plotted with correlation coefficient values of 1 and 0.8747 respectively. The results obtained confirms that Freundlich isotherm model is the most suitable model for the adsorption of copper ions by the layered double hydroxide. The thermodynamic parameters, $\Delta H°$ and $\Delta S°$ were calculated to predict the nature of adsorption. The negative values of $\Delta H°$ (-574 KJ/ mol) and the positive values of $\Delta S°$ (18.7 J/mol K) indicate that the adsorption process is spontaneous and exothermic in nature. The adsorption process followed pseudo-second-order kinetics, zero-order kinetic model and second-order kinetic model.

Keywords: Layered double hydroxide, Freundlich isotherm, Langmuir isotherm, Thermodynamics, Kinetics.

INTRODUCTION

Layered double hydroxides also known as hydrotalcite-like compounds or anionic clays, have received much attention in the past decades due to their wide spread applicability. Layered double hydroxide have positively charged layers of metal hydroxides and the anions and water molecules are located between the layers. The positive charges produce from the isomorphous substitution of divalent and trivalent cations are counter balanced by anions located between the layers[1]. Layered double hydroxides have a general formula of $[M^{2+}1_{-x}M^{3+}_x(OH)_2]$ $[An^{-x}/_{n·m}H_2O]$, where M^{2+} and M^{3+} are divalent and trivalent metal cations, respectively, A is the anions and x is the ratio $M^{3+}/(M^{2+} + M^{3+})^2$. The anions between the layers can be polymers, organic dyes, surfactants and organic acids[3]. Recently, layered double hydroxides have received considerable attention due to their anion-exchange capability. A variety of layered materials have been synthesized by different methods and layered double hydroxides have widespread applications as catalysts or catalyst precursors[4], adsorbents[5], anionic exchangers[6], in biochemistry[7], polymer additives[8] and as hybrid pigments[9]. Previous studies[10] have indicated that the thermostability of organic anions can be markedly improved after intercalation into the series of layered double hydroxides.

The flexibility of the inner core of layered double hydroxides has apparently made scientists and engineers place premium attention on their multiple uses including adsorption of heavy metals. Most recently, the use of layered double hydroxides as adsorbents for the removal of heavy metals in solution is also gaining prominence as shown by their studies[10-13]. The results of these studies indicated that layered double hydroxides are indeed very useful adsorbents. However, most of these studies used the intercalated forms of layered double hydroxides rather than the product from direct co-precipitation method, this is probably done to enhance the quality of crystals or adsorption capacity.

Heavy metals are a kind of toxin that frequently contaminates industrial and municipal wastewaters[14]. They result from a variety of industries, such as mining, plating, dyeing, electrochemical metal processing and battery storage, plus human activity[15]. Heavy metals are stable elements and cannot be degraded or eliminated[16,17]. Discharge of wastewater without appropriate treatment leads to residue and the accumulation of heavy metals in the environment. Heavy metals may be found in soil[16,18-23], earth's water, groundwater[24], sediments, plants[25] and even in dust[21]. They cause many health problems, including lung damage, renal damage, Wilson's disease (neurological or psychiatric symptoms of liver disease, compounded

with heavy metal deposits), insomnia, dermatitis, nausea, chronic asthma, headache, dizziness, rapid respiration, coughing, cancer, *etc.*[26,27]. In this study, we present our report on the synthesis of layered double hydroxides of magnesium and iron with a 2:1 ratio. These layered double hydroxide were characterized and employed in adsorption study of copper ion uptake in solution.

EXPERIMENTAL

Synthesis of Mg/Fe-CO₃: Carbonate form of Mg-Fe layered double hydroxide was synthesized by co-precipitation method. A 50 mL aqueous solution containing 0.3 M $Mg(NO_3)_2 \cdot 6H_2O$ and 0.1 M $Fe(NO_3)_3 \cdot 9H_2O$ with Mg/Fe ratios 2:1, was added drop wise into a 50 mL mixed solution of [NaOH (2 M) + Na_2CO_3 (1 M)] with vigorous stirring and maintaining a pH greater than 10 at room temperature. After complete addition which last between 2.5 to 3.0 h, the slurry formed was aged at 60 °C for 18 h. The products were centrifuged at 5000 rpm for 5 min, with distilled water 3-4 times and dried by freeze drying.

Characterization of layered double hydroxide: The powdered layered double hydroxide was characterized by powder X-ray diffraction (XRD), Fourier transform infrared spectroscopy (FTIR) and EDX/TEM analysis.

Preparation of metal solution: All reagents used for this study were analytical reagent grade and were procured from Zayo-Sigma Chemical Ltd. Jos, Nigeria. 1000 mg/L aqueous solutions of the metals ion was prepared as stock from their salts ($CuSO_4$). From the stock, working solutions of 0.08 g/L Cu, 0.12 g/L Cu and 0.16 g/L Cu were prepared from appropriate aliquots diluted to the appropriate concentration. The total concentration of the metal ion in aqueous solution was confirmed by analysis using (Unicamthermo/solar system 2009 model) atomic adsorption spectrometer (AAS).

Batch adsorption procedure: 0.2 g each of the powder samples was collected and weighed using an electronic weighing balance, the weighed sample was placed in three (3) pre-cleaned test tube. 10 mL of each metal ion solution with standard concentration of 0.08, 0.12 and 0.16 g/L which was made from spectroscopic grade standards of copper ion from copper sulphate were added to each test tube containing the weighed sample and equilibrated by rocking (agitation) for 0.5 h and then centrifuged at 2500 rpm for 5 min and decanted. The supernatants were stored for copper ion (Cu^{2+}) analysis as stated in metal analysis.

0.2 g each of the powder sample was weighed using an electronic weighing balance and placed in three (3) pre-cleaned test tube. 10 mL of the metal ion solution with standard concentration of 0.16 g/L which was made from spectroscopic grade standard of copper ion from copper nitrate was added to each test tube containing the weighed sample and equilibrated rocking (agitation) for each time intervals of 10, 20 and 30 min, respectively. The powered sample suspension were centrifuged for 5 min at 2500 rpm and decanted. The supernatants were stored for copper ion analysis as stated in metal analysis.

0.2 g each of the powder sample was collected and weighed using an electronic weighing balance; the weighed sample was placed in three pre-cleaned tubes. 10 mL of the metal ion solution with standard concentration of 0.16 g/L which was made from spectroscopic grade standard of lead ion from copper sulphate was added to each test tube containing the weighed sample and equilibrated rocking (agitation) for 1 h at temperatures of 40, 60 and 80 °C respectively using Gallenhamp water bath. This was immediately centrifuged at 2500 rpm for 5 min and then decanted. The supernatant were stored for copper ion analysis as stated in metal analysis.

Data analysis: The uptake of heavy metal ions was calculated from the mass balance, which was stated as the amount of solute adsorbed onto the solid. It equal the amount of solute removed from the solution. Mathematically can be expressed in eqn. 1[24]:

$$q_e = \frac{(C_o - C_e)}{S} \quad (1)$$

q_e: Heavy metal ions concentration adsorbed on adsorbent at equilibrium (mg of metal ion/g of adsorbent). C_o: Initial concentration of metal ions in the solution (mg/L). C_e: Equilibrium concentration or final concentration of metal ions in the solution (mg/L). S: Dosage concentration and it is expressed by eqn. 2:

$$S = \frac{m}{v} \quad (2)$$

where v is the initial volume of metal ions solution used (L) and m is the mass of adsorbent. The adsorption (%) was also calculated using eqn. 3:

$$\text{Adsorption (\%)} = \frac{C_o - C_e}{C_o} \times 100 \quad (3)$$

Equilibrium studies: Langmuir plots were carried out using the linearized eqn. 4 below

$$\frac{M}{x} = \frac{1}{abC_e} + \frac{1}{b} \quad (4)$$

where x is the amount of Cu^{2+} adsorbed per mass M of layered double hydroxide in mg/g, a and b are the Langmuir constants obtained from the slope and intercepts of the plots.

The essential characteristics of the Langmuir isotherm were expressed in terms of a dimensionless separation factor or equilibrium parameter S_f.

$$S_f = \frac{1}{1 + aC_o} \quad (5)$$

with C_o as initial concentration of Cu^{2+} in solution, the magnitude of the parameter S_f provides a measure of the type of adsorption isotherm. If $S_f > 1$, the isotherm is unfavourable; $S_f = 1$ (linear); $0 < S_f < 1.0$ (favourable) and $S_f = 0$ (irreversible).

The adsorption intensity of the Cu^{2+} in the carbon nanotube was assessed from the Freundlich plots using the linearized eqn. 6 below

$$\ln \frac{x}{M} = \frac{1}{n} (\ln C_e) + \ln K \quad (6)$$

where K and n are Freundlich constants and 1/n is approximately equal to the adsorption capacity.

The fraction of layered double hydroxide surface covered by the Cu^{2+} was computed using eqn. 7

$$\theta = 1 - \frac{C_e}{C_o} \qquad (7)$$

with θ as degree of surface coverage

Thermodynamics studies: The effectiveness of the adsorbent (layered double hydroxide) was assessed by the number of cycles of equilibrium sorption process required to reduce the levels of Cu^{2+} in solution according to the value of the distribution partition coefficient (K_d) in eqn. 8.

$$K_d = \frac{C_{aq}}{C_{ads}} \qquad (8)$$

where C_{aq} is concentration of Cu^{2+} (mg/g) in solution; C_{ads} is concentration of Cu^{2+} mg/L) in layered double hydroxides.

The apparent Gibbs free energy of sorption ΔG^o which is a fundamental criterion for spontaneity, was evaluated using the following equation

$$\Delta G^\circ = RT \ln k_d \qquad (9)$$

k_d is obtained from equation (eqn. 8).

The experimental data was further subjected to thermodynamic treatment in order to evaluate the apparent enthalpy (ΔH°) and entropy (ΔS°) of sorption using eqn. 10.

$$\Delta G^\circ = \Delta H^\circ - T\Delta S^\circ \qquad (10)$$

The isosteric heat of adsorption at constant surface coverage is calculated using the Clausius-Clapeyron equation:

$$\frac{d(\ln C_e)}{dT} = \frac{\Delta H^\circ}{RT^2} \qquad (11)$$

where, C_e is the equilibrium adsorbate concentration in the solution (mg L^{-1}), ΔHx is the isosteric heat of adsorption (kJ mol^{-1}), R is the ideal gas constant (8.314 J mol^{-1} K^{-1}) and T is temperature (K). Integrating the above equation, assuming that the isosteric heat of adsorption is temperature independent, gives the following equation:

$$\ln C_e = -\left(\frac{\Delta H_x}{R}\right)\frac{1}{T} + K \qquad (12)$$

where K is a constant.

The isosteric heat of adsorption is calculated from the slope of the plot of ln Ce *versus* 1/T different amounts of adsorbate onto adsorbent.

The linear form of the modified Arrhenius expression was applied to the experimental data to evaluate the activation energy (E_a) and sticking probability S* as shown in eqn. 13.

$$\ln(1-\theta) = S^* + \frac{E_a}{RT} \qquad (13)$$

The expression relating the number of hopping (n) and that of the surface coverage (θ) as shown in eqn. 14 was applied to the experimental data.

$$n = \frac{1}{(1-\theta)\theta} \qquad (14)$$

Kinetic studies: To determine the kinetic compliance of the experimental data, the results were subjected to the following kinetic models:

Zero-order kinetic model:

$$q_t = q_o + K_o t \qquad (15)$$

where; q_e and q_t are the amounts of the adsorbed metal ion (mg/g) at the equilibrium time and at any instant of time "t", respectively and k_o is the rate constant of the zero-order adsorption operation (l/min). Plotting of q_t *versus* t gives a straight line for the zero-order kinetics.

Second-order kinetic model:

$$\frac{1}{q_t} = \frac{1}{q_o} + K_2 t \qquad (16)$$

where, k_2 (min^{-1}) is the rate constant, q_o (mg g^{-1}) is the amount of Cu^{2+} adsorbed on surface at equilibrium, q_t (mg g^{-1}) is the amount of Cu^{2+} adsorbed on surface at time t (min).

Plotting of $1/q_t$ *versus* t gives a straight line for the second-order kinetics.

Pseudo-second order:

$$\frac{t}{q_t} = \frac{1}{h_o} + \frac{1}{q_e t} \qquad (17)$$

where, k_2 (min^{-1}) is the rate constant, h_o (mg g^{-1}) is the amount of Cu^{2+} adsorbed on surface at equilibrium, q_t (mg g^{-1}) is the amount of Cu^{2+} adsorbed on surface at time t (min).

The graph of t/q_t *versus* t gives a straight line for the pseudo-second-order model.

RESULTS AND DISCUSSION

SEM/EDX: FESEM/EDX was obtained using Carl Zeiss SMT supra 40 VPFESEM Germany and incapenta FET x 3 EDX, Oxford. It was operated at extra high tension (HT) at 5 kV and magnification at 20000X. FESEM uses electron to produce images (morphology) of samples and was attached with EDX for qualitative elemental analysis. Scanning electron microscope and energy dispersive spectroscope images of as-synthesized layered double hydroxides are presented in Figs. 1 and 2. The images show the surface morphology of the layered double hydroxides before and after adsorption studies. Scanning electron microscope image before adsorption studies [Fig. 1(a)] shows a heterogeneous/rough surface with several pores while the image after adsorption studies [Fig. 1(b)] show a smooth surface with several agglomeration of reacted hydroxide line. The smooth surface observed could be due to adsorbed metal ions filling the pores that existed before adsorption studies. The energy dispersive spectrograph before adsorption studies [Fig. 2(a)] show the presence of metal ions used in the synthesis of the layered double hydroxides such as aluminium, sodium and nickel and their percentage compositions. After adsorption studies, Fig. 5(b), the energy dispersive spectrograph, show the presence of copper ions adsorbed by the layered double hydroxide. Energy dispersive spectroscopy also shows that a chemical change has taken place during adsorption studies as observed in the elemental composition presented.

X-ray diffraction: X-ray diffraction (XRD) pattern of the sample was characterized by using a Shimadzu XRD-6000 diffractometer, with Ni-filtered Cu-K_α radiation (λ = 1.54 Å) at 40 kV and 200 mA. Solid samples were mounted on alumina
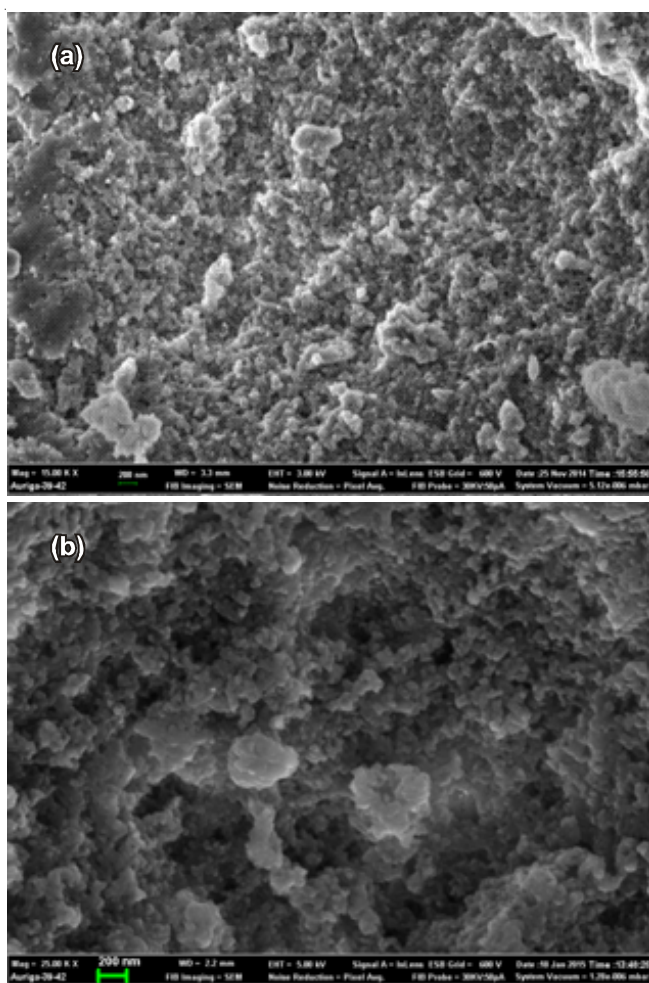
Fig. 1. Scanning electron microscope micrograph of Mg/Fe₂-CO₃ before (a) and after (b) adsorption studies
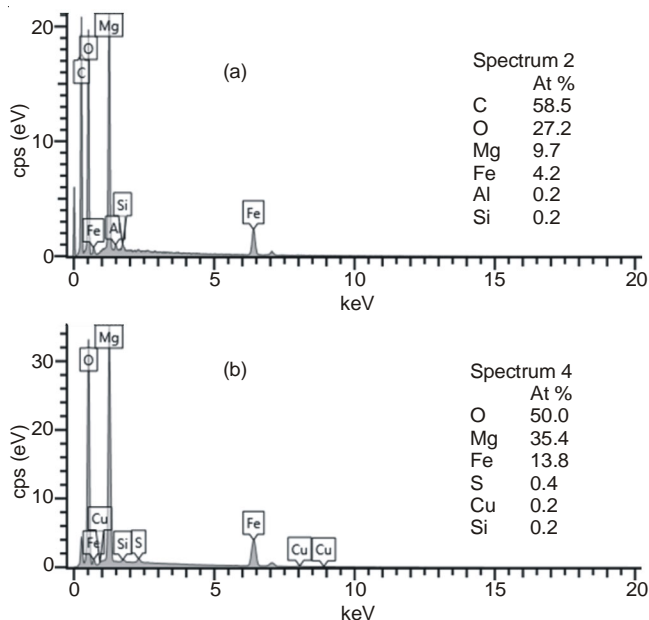

Fig. 2. Energy dispersive spectroscopy patterns of Mg/Fe₂-CO₃ pre (a) and post (b) adsorption energy dispersive spectroscopy

sample holder and basal spacing (d-spacing) was determined *via* powder technique. Samples scan were carried out at 10-60°, 2°/min at 0.003° steps.

The XRD patterns of Mg-Fe/CO₃ is shown in Fig. 3. The powder X-ray diffraction pattern of layered double hydroxide with Mg/Fe shows peaks at 2 theta degree 8.5°, 23° and 34.4° corresponding to basal spacing of 1.04, 0.772 and 0.258 respectively. The peaks at 45.8° and 59.6° are attributed to MgO.
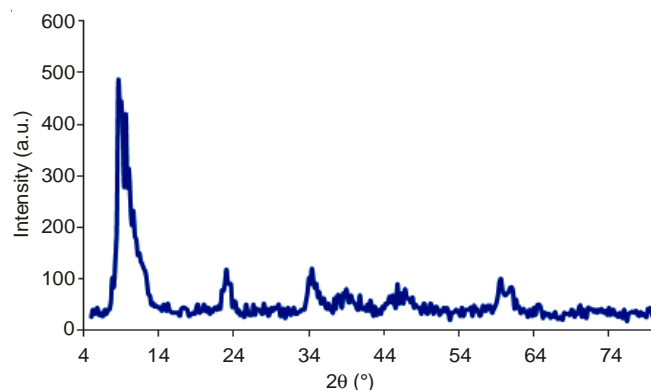
Fig. 3. Mg/Fe₂-CO₃ X-ray powder diffraction

FT-IR: FTIR spectrum was obtained using a Perkin Elmer 1725X spectrometer where samples will be finely ground and mixed with KBr and pressed into a disc. Spectrums of samples were scanned at 2 cm^{-1} resolution between 4000 and 400 cm^{-1}. As shown in Fig. 4, the band near 3400 cm^{-1} corresponds to the vibration bands of hydroxyls ν(OH). The bending mode of water molecules appears at 1738 cm^{-1} and the intensity increases slightly with increasing Mg/Fe ratio. The sharp intense band at 1355 cm^{-1} is the antisymmetric stretching of interlayer carbonate and the band at 678 cm^{-1} is due to ν(M-O) vibration.
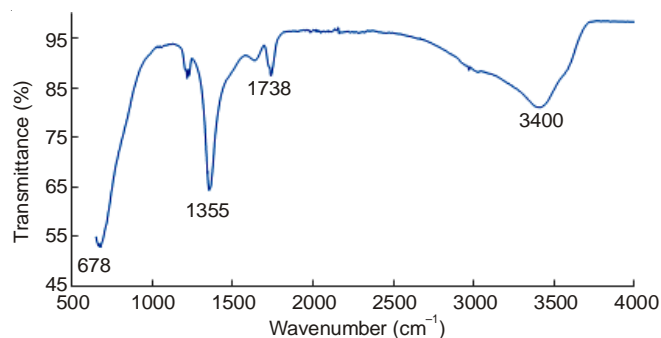

Fig. 4. Fourier transform infrared spectra of Mg/Fe₂-CO₃

Effect of temperature: Fig. 5 shows the effect of different temperatures 30, 60 and 80 and the percentage of metal removed from solution. It shows that there was a rapid adsorption from 0-30 °C after which there was a decrease in amount adsorbed.

Thermodynamics of adsorption: Isosteric heat of adsorption ΔH_x is one of the basic requirements for the characterization and optimization of an adsorption process and is a critical design variable in estimating the performance of an adsorptive separation process. It also gives some indication about the surface energetic heterogeneity. Knowledge of the heats of sorption is very important for equipment and process design. A plot of ln C_e against 1/T in Fig. 6 gives a slope equal
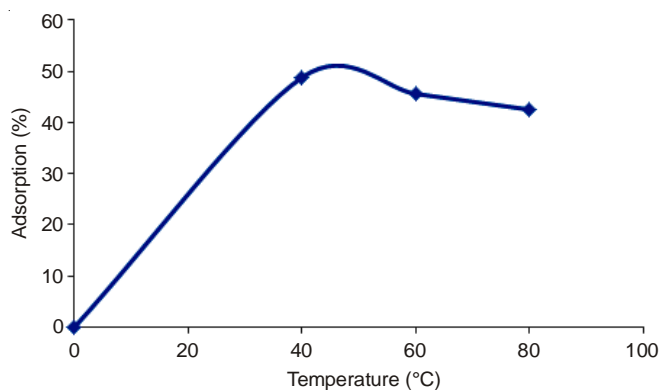
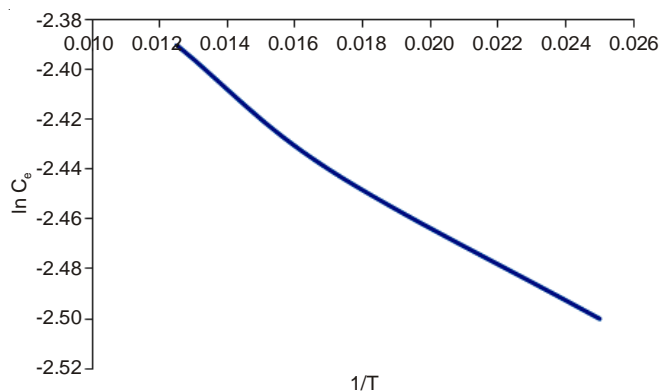Fig. 5. Effect of temperature on adsorption of Cu^{2+} onto layered double hydroxide

Fig. 6. Plot of ln C_e *vs.* 1/t for adsorption of Cu^{2+} onto layered double hydroxide

to ΔH_x. The value of ΔH_x derived from equation 12 was 19 KJ/mol which indicates that adsorption mechanism was physical adsorption and in an heterogeneous surface.

The activation energy E_a and the sticking probability S^* were calculated from eqn. 13. The value shown in Table-1 for E_a and S^* are 0.027 KJ/mol and 0.4, respectively (Fig. 7). The value of activation energy shows that the sorption process was a physical one since it is less than 4.2 KJ/mol. The sticking probability S^* indicates the measure of the potential of an adsorbate to remain on the adsorbent. It is often interpreted as $S^* > 1$ (no sorption), $S^* = 1$ (mixture of physico-sorption and chemisorption), $S^* = 0$ (indefinite sticking – chemisorption), $0 < S^* < 1$ (favourable sticking – physico-sorption).
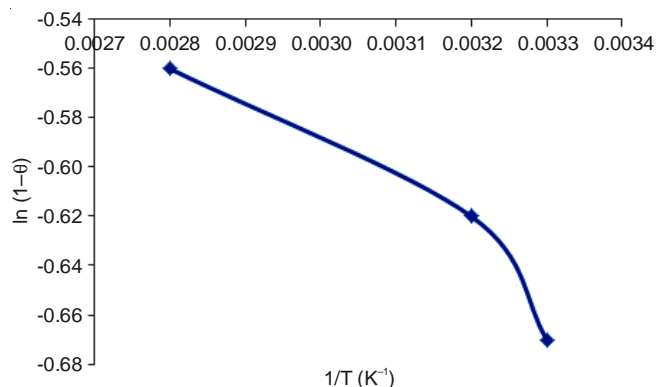

Fig. 7. Plot of ln (1-θ) *vs.* 1/T (K^{-1}) for the adsorption of Cu^{2+} onto layered double hydroxide

TABLE-1
THERMODYNAMIC PARAMETERS OF ADSORPTION OF LEAD ONTO LAYERED DOUBLE HYDROXIDE

Temp. (K)	$\Delta G°$ (KJ/mol)	$\Delta H°$ (KJ/mol)	$\Delta S°$ (J/mol K)	E_a (KJ/mol)	ΔH_x (KJ/mol)
313	0.133				
333	0.438	-5.74	18.8	0.027	19
353	0.880				

The probability of Cu^{2+} finding vacant site on the surface of the layered double hydroxide during the sorption was correlated by the number of hopping (n) done by the Cu^{2+} is calculated from eqn. 14. The hopping number presented in Table-1 is 4. The lower the hopping number, the faster the adsorption. The low value of n obtained in this study suggests that the adsorption of Cu^{2+} on the layered double hydroxide was very fast.

Table-1 also presents the Gibbs free energy $\Delta G°$ for the sorption of Cu^{2+} by the layered double hydroxide which was calculated from eqn. 9. Gibbs free energy is the fundamental criterion of spontaneity. The $\Delta G°$ values from the experimental data are 0.133, 0.438 and 0.880 KJ/mol this indicate that the adsorption process was spontaneous. The values of the enthalpy change ($\Delta H°$) and entropy change ($\Delta S°$) were calculated from eqn. 10 to be -5.74 KJ/mol and 18.7 J/molK respectively as shown in Fig. 8. A plot of $\Delta G°$ against T gives a straight line graph with slope and intercept defining the $\Delta H°$ and $\Delta G°$. A negative $\Delta H°$ suggests that sorption proceeded favourably at a lower temperature and the sorption mechanism was exothermic. A positive ΔS suggests that the freedom of the adsorbed Cu^{2+} was not restricted in the layered double hydroxide, indicating that physico-sorption mechanism predominates.
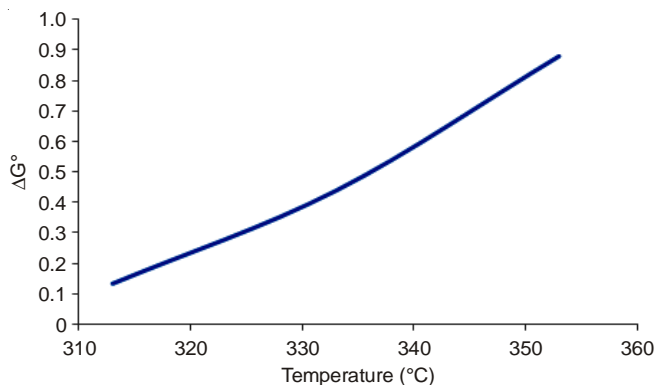

Fig. 8. Plot of $\Delta G°$ *vs.* temperature for adsorption of Cu^{2+} onto layered double hydroxide

Kinetic studies

Effect of time: Adsorption increased steadily from 10-30 min as shown in Fig. 9. This implies that adsorption is dependent on contact time.

The experimental data were fitted to zero-order kinetic model, second-order kinetic model and pseudo-second order model with regression correlation coefficient values of 0.9796, 0.9592 and 0.9994 respectively as shown in Figs. 10-12. The results (Table-2) shows that the best fit for the adsorption of copper ions by the layered double hydroxide was pseudo second-order models.

TABLE-2
KINETIC PARAMETERS OF ADSORPTION OF COPPER(II) BY Mg/Fe-CO$_3$

Zero-order kinetic model			Second-order kinetic model			Psuedo-second order model		
K$_o$	q$_o$	R^2	K$_2$	q$_o$	R^2	h$_o$	q$_e$	R^2
0.3	0.004	0.9796	3.2	-35.7	0.9592	0.48	0.12	0.9994
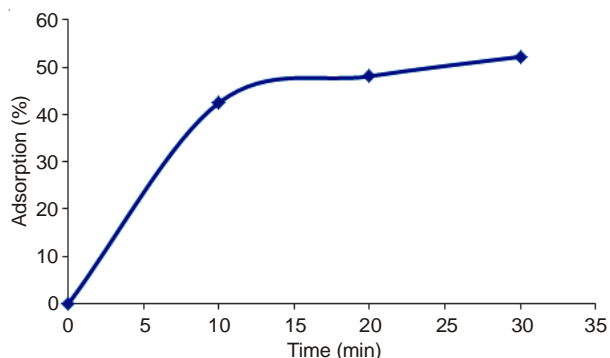
Fig. 9.   Effect of contact time on adsorption of Cu^{2+} onto layered double hydroxide
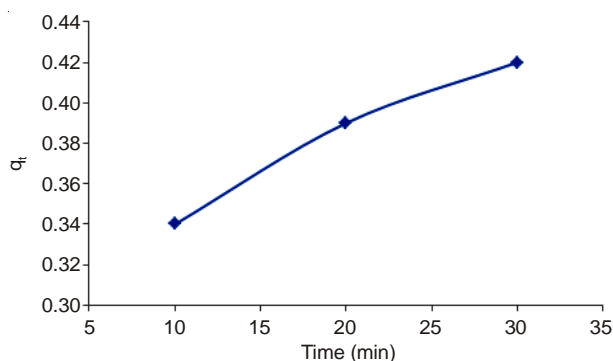
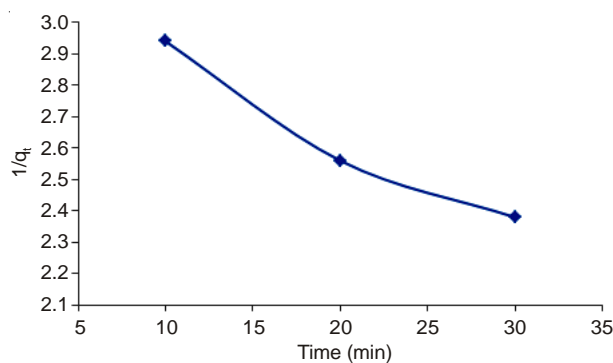Fig. 10. Plot of q$_t$ *vs.* t for adsorption of Cu^{2+} onto layered double hydroxide

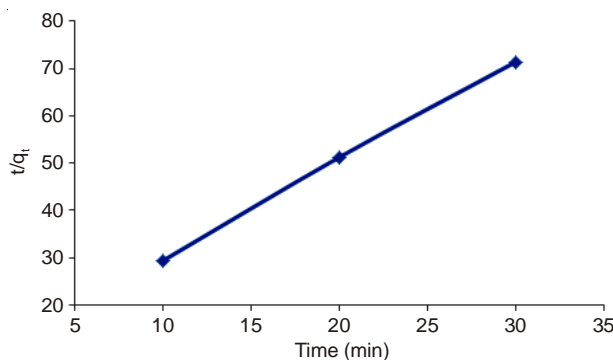Fig. 11. Plot of 1/q$_t$ *vs.* t for adsorption of Cu^{2+} onto layered double hydroxide

Fig. 12. Plot of t/q$_t$ *vs.* t for adsorption of Cu^{2+} onto layered double hydroxide

Effect of concentration: The percentage sorption of Cu^{2+} by the layered double hydroxide at different concentrations of the Cu^{2+} is presented in Fig. 13. The maximum adsorption of 57.5% took place at equilibrium concentration of 0.08 g/L Cu^{2+}. This is because at lower concentration more layered double hydroxide pore spaces were available for the Cu^{2+} but as the concentration of Cu^{2+} increased, the adsorption capacity of the layered double hydroxide decreased due to reduced availability of free pore spaces. The results indicated that the sorption of Cu^{2+} were very much dependent on the concentration of the Cu^{2+}.
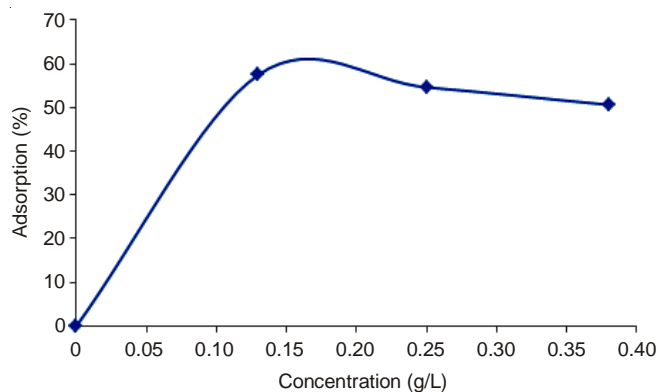

Fig. 13. Effect of concentration on adsorption of Cu^{2+} onto layered double hydroxide

Isotherm studies: Fig. 14 shows the Langmuir isotherm plot of adsorption of copper ions by layered double hydroxide. The result shows (Table-3) a skewed line and therefore, the experimental data did not fit the isotherm model properly.
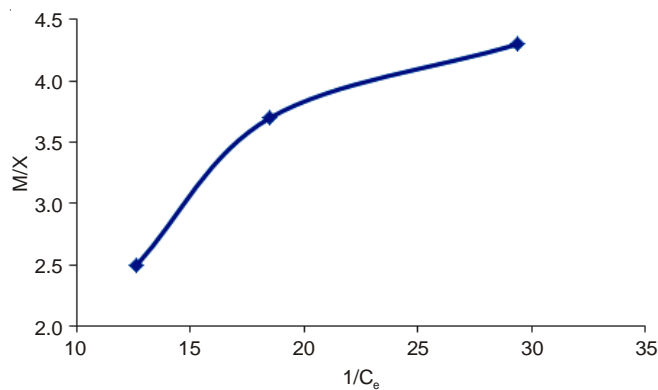

Fig. 14. Langmuir isotherm plot for adsorption of Cu^{2+} on layered double hydroxide

TABLE-3
ISOTHERM PARAMETERS OF LANGMUIR AND FREUNDLICH

Freundlich constants			Langmuir constants		
K	n	R^2	a	b	R^2
2.1	0.905	1	0.069	9.921	0.8747

In determining the nature of the adsorption process, whether favourable or unfavourable, the dimensionless constant separation term S_f was investigated (eqn. 3). The result $S_f = 0.989$ was less than one and greater than zero which showed that the sorption of Cu^{2+} onto the layered double hydroxide was favourable.

The experimental data was further fitted in to confirm its applicability to the Freudlich model, the result as shown in Fig. 15 fitted perfectly (Table-3). The adsorption capacity which is calculated from the slope of the graph is 0.905, less than one.
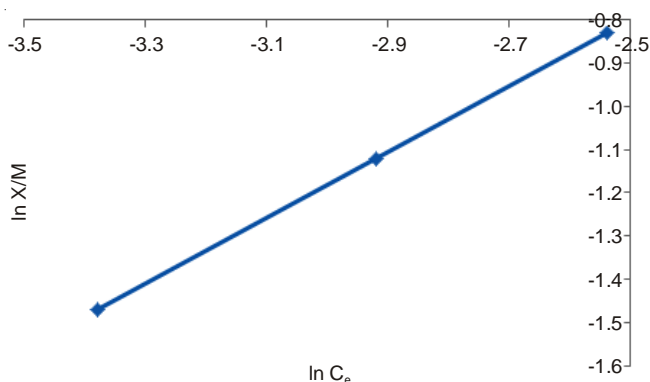

Fig. 15. Freundlich Isotherm plot for adsorption of Cu^{2+} on layered double hydroxide

Conclusion

Mg-Fe-layered double hydroxide is a material with high potential for the removal of copper from aqueous solution. The batch adsorption experimental data shows that the entire adsorption process is dependent on temperature and not on concentration and time. The kinetic data were fitted to zero-order kinetic model, second order kinetic model, pseudo second-order model and shows that pseudo second-order model best describe the adsorption kinetics. Again the data was also subjected to both Langmuir and Freudlinch isotherm models with Freundlich fitting the best isotherm. The negative value of $\Delta H°$ (-5.74 KJ/mol) indicate that the process is endothermic and a given amount of heat is evolve during the binding of copper ions on the surface of the layered double hydroxide while the positive value of $\Delta S°$ (18.7 J/molK) indicate an increase in the degree of freedom of the adsorbed specie.

REFERENCES

1. L.C. Hsu, S.L. Wang, Y.M. Tzou, C.F. Lin and J.H. Chen, *J. Hazard. Mater.*, **142**, 242 (2007).
2. Q. Hu, Z. Xu, S. Qiao, F. Haghseresht, M. Wilson and G.Q. Lu, *J. Colloid Interf. Sci.*, **308**, 191 (2007).
3. R. Roto, F. Nindiyasari and I. Tahir, *J. Phys. Sci.*, **20**, 73 (2009).
4. N. Karapinar and R. Donat, *Desalination*, **249**, 123 (2009).
5. J.P. Landaburu-Aguirre, E. Pongrácz, P. Perämäki and R.L. Keiski, *J. Hazard. Mater.*, **180**, 524 (2010).
6. I. Pavlovic, M.R. Perez, C. Barriga and M.A. Ulibarri, *Appl. Clay Sci.*, **43**, 125 (2009).
7. M.A. Woo, T. Woo Kim, M.-J. Paek, H.-W. Ha, J.-H. Choy and S.-J. Hwang, *J. Solid State Chem.*, **184**, 171 (2011).
8. M. Badreddine, A. Legrouri, A. Barroug, A. De Roy and J.P. Besse, *Mater. Lett.*, **38**, 391 (1999).
9. F.L. Melquiades, P.S. Parreira, C.R. Appoloni, W.D. Silva and F. Lopes, *Appl. Radiat. Isot.*, **69**, 327 (2011).
10. A. Demirba, *J. Hazard. Mater.*, **157**, 220 (2008).
11. Z. Hamzah, M.N.A. Rahman, Y. Yasin, S.M. Sumari and A. Saat, *J. Nucl. Relat. Technol.*, **8**, 60 (2011).
12. J. Gong, T. Liu, X. Wang, X. Hu and L. Zhang, *Environ. Sci. Technol.*, **45**, 6181 (2011).
13. G.N. Pshinko, *J. Chem.*, Article ID 347178 (2013).
14. M.R. Pérez, I. Pavlovic, C. Barriga, J. Cornejo, M.C. Hermosin and M.A. Ulibarri, *Appl. Clay Sci.*, **32**, 245 (2006).
15. K. Kadirvelu, K. Thamaraiselvi and C. Namasivayam, *Bioresour. Technol.*, **76**, 63 (2001).
16. W. Shi, H. Shao, H. Li, M. Shao and S. Du, *J. Hazard. Mater.*, **170**, 1 (2009).
17. R. Vinodh, R. Padmavathi and D. Sangeetha, *Desalination*, **267**, 267 (2011).
18. K. Loska, D. Wiechu³a and I. Korus, *Environ. Int.*, **30**, 159 (2004).
19. K. Zhao, X. Liu, J. Xu and H.M. Selim, *J. Hazard. Mater.*, **181**, 778 (2010).
20. J. Bai, R. Xiao, A. Gong, H. Gao and L. Huang, *Chem. Earth*, **36**, 447 (2011).
21. B. Wei and I. Yang, *Microchem. J.*, **94**, 99 (2010).
22. V. Ramachandran and T.J. D'souza, *Water Air Soil Pollut.*, **111**, 225 (1999).
23. G. Yaylali-Abanuz, *Microchem. J.*, **99**, 82 (2011).
24. F. Guzel, H. Yakut and G.J. Topal, *J. Hazard. Mater.*, **153**, 1275 (2008).
25. A. Dube, R. Zbytniewski, T. Kowalkowski, E. Curkrowska and B. Buszewski, *Pol. J. Environ. Stud.*, **10**, 1 (2001).
26. A.K. Meena, G.K. Mishra, P.K. Rai, C. Rajagopal and P.N. Nagar, *J. Hazard. Mater.*, **122**, 161 (2005).
27. F. Cavani, F. Trifiro and A. Vaccari, *Catal. Today*, **11**, 173 (1991).